OKINAWA INSTITUTE OF SCIENCE AND TECHNOLOGY GRADUATE UNIVERSITY
沖縄科学技術大学院大学

Shubnikov-de-Haas oscillation and possible modification of effective mass in CeTe3 thin films

Shubnikov-de-Haas oscillation and possible modification of effective mass in CeTe₃ thin films

Mori Watanabe, Ryoya Nakamura, [iD] Sanghyun Lee, Takuya Asano, Takashi Ibe, Masashi Tokuda, Hiroki Taniguchi, Daichi Ueta, [iD] Yoshinori Okada, [iD] Kensuke Kobayashi, and [iD] Yasuhiro Niimi

COLLECTIONS

Paper published as part of the special topic on 65th Annual Conference on Magnetism and Magnetic MaterialsMMM2021, 65th Annual Conference on Magnetism and Magnetic MaterialsMMM2021, 65th Annual Conference on Magnetism and Magnetic MaterialsMMM2021, 65th Annual Conference on Magnetism and Magnetic MaterialsMMM2021 and 65th Annual Conference on Magnetism and Magnetic MaterialsMMM2021

View Online   Export Citation   CrossMark

ARTICLES YOU MAY BE INTERESTED IN

Quantum oscillations with magnetic hysteresis observed in CeTe₃ thin films
Applied Physics Letters **117**, 072403 (2020); https://doi.org/10.1063/5.0007517

Precession coupled spin current in spin torque driven magnetic tunnel junctions
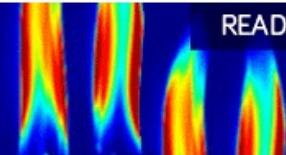AIP Advances **11**, 015006 (2021); https://doi.org/10.1063/9.0000020

Hydrogel: A potential therapeutic material for bone tissue engineering
AIP Advances **11**, 010701 (2021); https://doi.org/10.1063/5.0035504

Shubnikov-de-Haas oscillation and possible modification of effective mass in CeTe₃ thin films

View Online   Export Citation   CrossMark

Mori Watanabe,[1,a] **Ryoya Nakamura,**[1] **Sanghyun Lee,**[1] (ID) **Takuya Asano,**[1] **Takashi Ibe,**[1] **Masashi Tokuda,**[1] **Hiroki Taniguchi,**[1] **Daichi Ueta,**[2] **Yoshinori Okada,**[2] (ID) **Kensuke Kobayashi,**[1,3] (ID) **and Yasuhiro Niimi**[1,4,b] (ID)

AFFILIATIONS

[1] Department of Physics, Graduate School of Science, Osaka University, Toyonaka, Osaka 560-0043, Japan
[2] Okinawa Institute of Science and Technology Graduate University, Okinawa 904-0495, Japan
[3] Institute for Physics of Intelligence and Department of Physics, The University of Tokyo, Bunkyo-ku, Tokyo 113-0033, Japan
[4] Center for Spintronics Research Network, Osaka University, Toyonaka, Osaka 560-8531, Japan

Note: This paper was presented at the 65th Annual Conference on Magnetism and Magnetic Materials.
[a] **Author to whom correspondence should be addressed:** watanabe@meso.phys.sci.osaka-u.ac.jp
[b] **Electronic mail:** niimi@phys.sci.osaka-u.ac.jp

ABSTRACT

Magnetoresistance measurements have been performed in CeTe₃ thin film devices in a temperature range from 2.1 to 20 K up to 8 T. A clear Shubnikov-de-Haas oscillation was observed in the whole temperature range. The temperature dependence of the oscillation amplitude was found to deviate from the Lifshitz–Kosevich formula below the magnetic transition temperature at $T_{N1} \approx 3$ K. This indicates a significant interplay between the magnetic ordering and the conduction electrons, which could lead to a modification of the effective cyclotron mass. By analyzing the temperature dependence of the oscillation amplitude, we have estimated the effective mass, quantum lifetime and quantum mobility of the material both in the paramagnetic and antiferromagnetic states.

In recent years, van-der-Waals (vdW) materials have been attracting much attraction in the field of magnetism. This is due to the recent discovery of vdW ferromagnets, which have been found to retain its magnetic order even when the dimensionality is lowered, even down to the atomic monolayer limit.[1–4] These materials allow application of electronic gating. For example, the magnetic transition temperatures can be tuned by gating even above room temperature.[5–9] Furthermore, advanced stacking techniques allow fabrication of multilayer spintronic devices with unique proximity and interface effects.[10–13]

In the emergence of these vdW ferromagnets, extending our understanding to vdW antiferromagnets (AFM) is an important task. Fundamentally, many interesting phenomena are theorized to arise from low-dimensional AFMs, such as spin liquid states and Kosterlitz–Thouless transition.[14–16] However, experimental studies had mostly been limited to bulk materials with pseudo-2D

conduction, with the exception of liquid helium. Exploration of vdW AFMs would allow experimental research of various AFM spin systems down to its monolayer limit. Furthermore, the thin film fabrication allows implementation of antiferromagnets to spintronic devices,[17–21] which is a promising candidate for fast and robust devices compared to the ferromagnetic counterpart.

We focus on a vdW antiferromanget CeTe₃, which is a material in the family of rare earth tritellurides RTe₃ (R = Lanthanoid). This family of materials have been studied extensively in bulk for its charge density wave formation.[22–25] In spite of the existence of partial gaps in the momentum space, these materials possess highly metallic conduction due to the Te bilayers, allowing electrical transport measurements to be performed.[26] Within this family of materials, CeTe₃ also has two magnetic transitions at $T_{N1} \approx 3.0$ K and $T_{N2} \approx 1.2$ K. The first transition at T_{N1} is from a paramagnetic state to a possibly short-range AFM state with an in-plane easy axis. The

second transition at T_{N2} is from the short-range AFM state to a long-range AFM order with an in-plane easy axis which is nonparallel to the first AFM transition.[27] CeTe$_3$ possesses interesting magnetic properties owing to the magnetic moment at the Ce site, as shown in Fig. 1(a). Specifically, it has recently been reported that quantum fluctuation can be induced systematically CeTe$_3$ by doping Se, leading to a different magnetic order with an out-of-plane easy axis.[28] Studies of CeTe$_3$ thin films and Se-doped counterpart may elucidate roles of quantum fluctuation in atomically thin AFMs, and the enhanced quantum fluctuation in thin films could lead to observation of quantum critical behaviour. However, the above results are from the bulk structure, and thin film transport measurements had not been performed so far. In our previous paper,[29] we reported successful electrical transport measurements of CeTe$_3$ thin film devices. Clear Shubnikov-de-Haas (SdH) oscillations were observed in a temperature range between 0.4 and 4 K, and the analysis of the oscillation indicated possible deformation of the Fermi surface below $T_{N2} \approx 1.2$ K. A weak magnetic hysteresis was also observed below T_{N1}, indicating a possible canting of the magnetic moments due to the thin film fabrication. On the other hand, we were not able to report detailed measurements above T_{N1} in the previous paper due to the measurement setup.[29] The temperature T dependence of SdH oscillation above T_{N1} is highly desired, as this would allow determination of the conduction electron properties, such as the effective cyclotron mass, quantum lifetime and mobility.

In this paper, we report magnetotransport measurements of 40 – 100 nm thick CeTe$_3$ devices in a temperature range from 2.1 to 20 K. Specifically, we have observed a low frequency SdH oscillation with a frequency of 34 T, which occupies roughly 0.15% of the entire Brillouin zone. Such a small Fermi pocket likely exists due to the Fermi surface reconstruction along with the charge density wave formation. We then performed fast Fourier transformation (FFT) for the observed oscillation, in order to analyze the temperature dependence of the oscillation amplitude. A rapid enhancement of the oscillation amplitude was observed below the first magnetic transition temperature T_{N1}. In other words, the oscillation amplitude deviates from the Lifshitz–Kosevich (LK) formula below T_{N1}. The result indicates that the effective cyclotron mass could be enhanced due to the interaction between the conduction electrons and the magnetic order.

The thin film device was fabricated through the procedures outlined in our previous report.[29] First, CeTe$_3$ thin flakes were mechanically exfoliated onto SiO$_2$/Si substrates using scotch tape. Polymethyl-methacrylate (PMMA) resist was then spincoated onto the substrates, and electrodes were patterned by using electron beam lithography. After the development, Au electrodes were obtained onto the CeTe$_3$ flakes through resistive heating vapor deposition and subsequent lift-off process in acetone. It should be noted that the device is sensitive to ambient air, and the quality deteriorates within a few days. Therefore, all the fabrication processes have been performed in a glovebox filled with 99.9999% Ar. The device was also capped with PMMA after the liftoff process, in order to avoid any further oxidization. The device was cooled using a commercial ^{4}He cryostat system with a superconducting magnet. Electrical transport measurements were performed through the standard 4-probe method using a Lock-in amplifier.

In Fig. 1(b), we show the temperature dependence of the resistivity $\rho(T)$ of the device from 2.1 K up to 300 K, from which we can
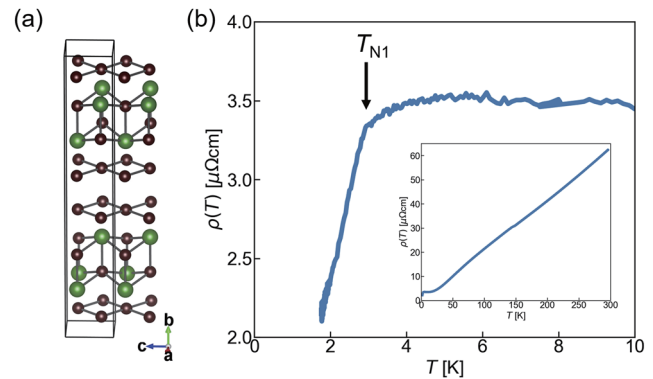

FIG. 1. (a) Crystal structure of CeTe$_3$. Green and brown spheres represent Ce and Te atoms, respectively. (b) Temperature dependence of the resistivity $\rho(T)$. The sharp drop in $\rho(T)$ indicates the magnetic transition temperature at $T_{N1} \approx 3$ K. The inset in (b) shows the temperature dependence of $\rho(T)$ from room temperature.

estimate the magnetic transition temperature as well as the device quality. As already demonstrated in our previous measurements,[29] the $\rho(T)$ curve resembles that of bulk CeTe$_3$, with a sharp drop at the antiferromagnetic transition temperature $T_{N1} \approx 3$ K. The residual resistivity ratio (RRR) at $T \approx 2.1$ K resulted in a value of 29.

Next, we measured magnetoresistance (MR) $\rho(B)$ up to a magnetic field B of 8 T in a temperature range from 2.1 to 20 K. The magnetic field was applied along the b-axis of the crystal, i.e., perpendicular to the plane [see Fig. 1(a)]. Figure 2 shows the MR with $\rho(B = 0)$ subtracted, i.e., $\Delta\rho \equiv \rho(B) - \rho(B = 0)$. A clear SdH oscillation was observed in the whole temperature range. The amplitude of the oscillation decreases with increasing temperature. We note that the absolute amplitude of the SdH oscillation was smaller than our previous measurements.[29] This is likely due to the device quality, as the RRR of the present device is roughly half, compared
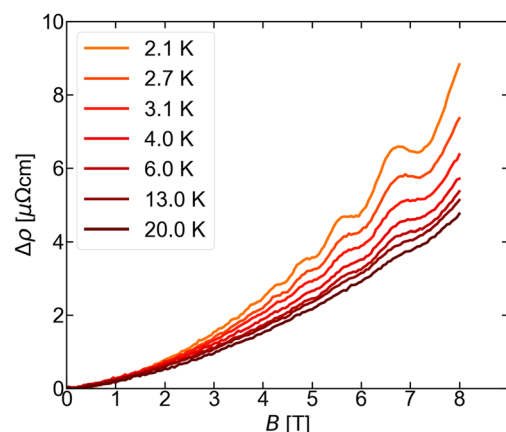

FIG. 2. MR measurements of the 100 nm thick CeTe$_3$ thin film from 2.1 K up to 20 K. The magnetic field was applied parallel to the b-axis of the crystal.
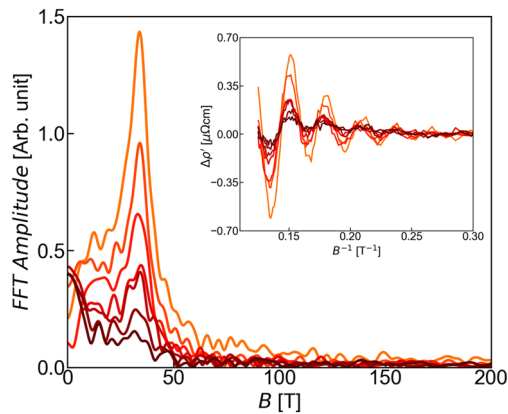
FIG. 3. FFT of the SdH oscillation of the 100 nm thick CeTe$_3$ device at different temperatures. The color labels are the same as in Fig. 2. The inset shows $\Delta\rho'$ versus the inverse of the applied field. The oscillatory part $\Delta\rho'$ of the MR has been extracted through subtraction of polynomial background for $\Delta\rho$ in Fig. 2.

to the previous devices. However, a clear quantum oscillation persists over a relatively wide range of temperatures, enabling detailed analysis.

SdH oscillations are periodic to the inverse of the applied field, and the temperature dependence of the oscillation amplitudes provides insight into the characteristics of the conduction electrons present in the material. Therefore, we have plotted the observed SdH oscillation as a function of the inverse of B and performed FFT, as shown in Fig. 3. A single frequency peak has been obtained at 34 T. The FFT amplitude decreases as the temperature is increased. This result is consistent with our previous work:[29] the low frequency quantum oscillation occupies only 0.15% of the entire Brillouin zone, which likely originates from Fermi surface deformation due to the incommensurate charge density wave periodicity. The existence

of a small Fermi pocket has been observed in a number of rare-earth tritellurides with charge density wave formation, including GdTe$_3$[26] and LaTe$_3$,[30] and it seems to be a relatively common feature that exists in the conduction at the Telluride bilayers. In general, SdH oscillations are described using the LK equation,

$$\Delta\rho' \propto \frac{\lambda(B)T}{\sinh(\lambda(B)T)} e^{-\lambda(B)T_D} \cos\left\{2\pi\left(\frac{F}{B} - \frac{1}{2} + \beta + \delta\right)\right\}, \quad (1)$$

where $\Delta\rho'$ is the oscillatory part of MR, T_D is the Dingle temperature, F is the frequency, $2\pi\beta$ is the Berry phase, and δ is a phase shift which is 0 and $\pm\frac{1}{8}$ for 2D and 3D systems, respectively. $\lambda(B) = (2\pi^2 k_B m^*)/(\hbar e B)$, where k_B is the Boltzmann constant, m^* is the effective cyclotron mass, $\hbar$ is the reduced Plank's constant, and e is the elementary charge. At a constant applied field B_0, the amplitude of the SdH oscillation attenuates as a function of T with a factor of $\lambda(B_0)T/\sinh(\lambda(B_0)T)$, and a fit of this function to the FFT amplitude allows for the estimation of the effective cyclotron mass of the electron. The mean value of the analyzed magnetic field range $B_0 \approx 5.5$ T was used for the FFT fit.

Figure 4(a) shows the temperature dependence of the FFT amplitude for different devices. First, we discuss the behavior observed for the 100 nm thick device. At temperatures above T_{N1}, the FFT amplitude follows the attenuation behavior described in the LK formula. Meanwhile, the behavior deviates below the magnetic transition temperature T_{N1}, with FFT amplitudes rapidly increasing roughly by a factor of 3 in a temperature range between 2.1 and 4 K. The deviation from the LK formula below T_{N1} has also been observed previously in related materials such as GdTe$_3$, however its behavior is notably different. In GdTe$_3$,[26] the FFT amplitude was observed to reach a plateau under its magnetic transition temperature. On the other hand, a rapid enhancement of the FFT amplitude was observed below T_{N1} in CeTe$_3$. In the temperature dependent attenuation function of the LK formula [i.e., the prefactor of Eq. (1)], the only free parameter is the effective cyclotron
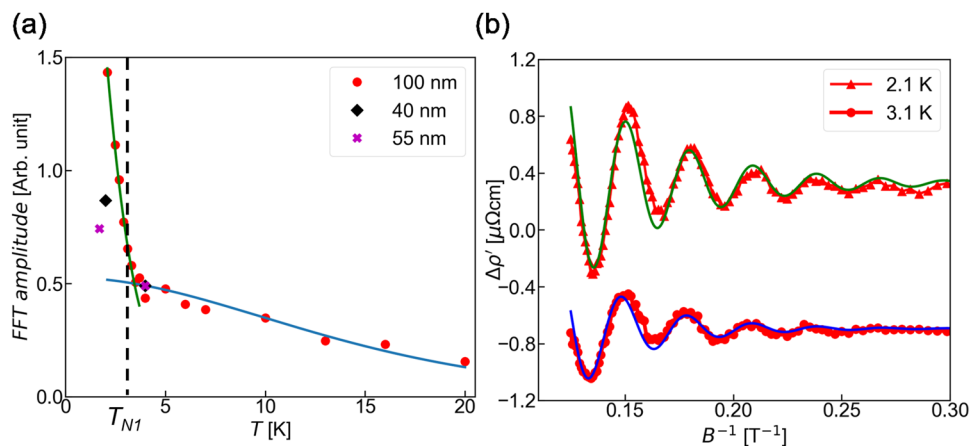

(a) **(b)**

FIG. 4. (a) Temperature dependence of the FFT amplitude. The green and blue lines show the best fits to the temperature dependent part of the LK formula below and above the magnetic transition temperature for the 100 nm thick CeTe$_3$ device. Different markers show the FFT amplitudes for devices of two different thicknesses (40 and 55 nm). The amplitudes were normalized by the amplitude of the LK fit for the 100 nm device at 4 K. (b) Refitting of the LK formula to the data at T = 2.1 (triangle) and 3.1 K (circle), respectively. The vertical axis is shifted for clarity.

mass. Therefore, the natural conclusion would be that the effective cyclotron mass of the conduction electrons are somehow modified due to the interaction between the magnetic ordering of CeTe$_3$ and the conduction electron. Therefore, a separate fit of the attenuation function has been made for temperatures below T_{N1}. The green and blue curves shown in Fig. 4(a) are the fits to the attenuation function below and above $T_{N1} \approx 3$ K for the 100 nm thick device. It should be noted that this enhancement of the amplitude below T_{N1} is reproducible with multiple devices of different thicknesses (40 and 55 nm). For both devices, the FFT amplitude is enhanced below T_{N1} roughly by a factor of 2, clearly deviating from the paramagnetic fit.

Using least squares fitting to the attenuation function, the effective cyclotron mass m^* can be obtained: above T_{N1}, $m^* \approx 0.061 m_e$ and below T_{N1}, $m^* \approx 0.43 m_e$ where m_e is the electron rest mass. Interestingly, m^* is enhanced by a factor of 7 below T_{N1}. One possibility for the origin of the enhancement could be attributed to the strong RKKY interaction in CeTe$_3$.[31,32] The conduction electrons could be bound near the Ce sites due to the strong RKKY interaction, resulting in an enhanced effective mass, although further study is required to fully explain this phenomenon. With an estimate of the effective mass, the oscillatory part of the MR can be refitted by the LK formula, as shown in Fig. 4(b). From this fitting, we can estimate the Dingle temperature T_D and the phase shift $\beta + \delta$. $\beta + \delta$ provides information about the topology of the band structures, while T_D enables us to calculate quantum lifetime and mobility, i.e., how much the conduction electrons are scattered and how well defined the Landau levels are. We obtain $T_D = 32$ K and $\beta + \delta = 1.1$ for 3.1 K, and $T_D = 2.2$ K and $\beta + \delta = -0.13$ for 2.1 K. The value of $\beta + \delta$ is close to 1 or 0 in both paramagnetic and antiferromagnetic states, which indicates a Berry phase of 2π and a topologically trivial band structure. The estimations of quantum lifetime and mobility given as $\tau_q = \hbar/(2\pi k_B T_D)$ and $\mu_q = e\tau_q/m^*$ respectively are 3.8×10^{-14} s and 1100 cm^{2}V^{-1}s^{-1} for the paramagnetic state and 5.5×10^{-13} s and 2300 cm^{2}V^{-1}s^{-1} for the antiferromagnetic state. These values are quantitatively consistent with those of bulk GdTe$_3$[26] with the mobility of $1200 - 2000$ cm^{2}V^{-1}s^{-1}. Although the effective cyclotron mass increased under the antiferromagnetic state, T_D decreased under the magnetic order, resulting in a larger quantum lifetime and mobility in the antiferromagnetic state compared to the paramagnetic state. The increase in the mobility of the electrons possibly originates from the loss of paramagnetic scattering, also observed as a large drop in $\rho(T)$ below T_{N1} [see Fig. 1(b)].[32]

In conclusion, we have performed MR measurements on $40 - 100$ nm thick CeTe$_3$ devices in a temperature range from 2.1 to 20 K. A clear SdH oscillation was observed in the whole temperature range. From the FFT analysis, we found a single frequency peak at $B = 34$ T. The temperature dependence of the FFT amplitude was found to deviate below the magnetic transition temperature T_{N1}, indicating modification of the conduction electron effective mass below T_{N1}. Therefore, the effective mass was estimated independently at the paramagnetic state and antiferromagnetic state. Based on this assumption, we obtain $m^* = 0.061 m_e$ in the paramagnetic state and $m^* = 0.43 m_e$ in the antiferromagnetic state. This could be attributed to the strong RKKY interaction present in CeTe$_3$. Meanwhile, the quantum mobility was estimated to be 1100 cm^{2}V^{-1}s^{-1} for the paramagnetic state and 2300 cm^{2}V^{-1}s^{-1} for the antiferromagnetic state. The increase in mobility below T_{N1} could be linked

to the large loss of paramagnetic scattering in the antiferromagnetic state.

DATA AVAILABILITY

The data that support the findings of this study are available from the corresponding author upon reasonable request.

REFERENCES

[1] B. Huang, G. Clark, E. Navarro-Moratalla, D. R. Klein, R. Cheng, K. L. Seyler, D. Zhong, E. Schmidgall, M. A. McGuire, D. H. Cobden, W. Yao, D. Xiao, P. Jarillo-Herrero, and X. Xu, Nature **546**, 270 (2017).

[2] C. Gong, L. Li, Z. Li, H. Ji, A. Stern, Y. Xia, T. Cao, W. Bao, C. Wang, Y. Wang, Z. Q. Qiu, R. J. Cava, S. G. Louie, J. Xia, and X. Zhang, Nature **546**, 265 (2017).

[3] D. J. O'Hara, T. Zhu, A. H. Trout, A. S. Ahmed, Y. K. Luo, C. H. Lee, M. R. Brenner, S. Rajan, J. A. Gupta, D. W. McComb, and R. K. Kawakami, Nano Lett. **18**, 3125–3131 (2018).

[4] Z. Fei, B. Huang, P. Malinowski, W. Wang, T. Song, J. Sanchez, W. Yao, D. Xiao, X. Zhu, A. F. May, W. Wu, D. H. Cobden, J. Chu, and X. Xu, Nat. Mater. **17**, 778 (2018).

[5] Y. Deng, Y. Yu, Y. Song, J. Zhang, N. Z. Wang, Z. Sun, Y. Yi, Y. Z. Wu, S. Wu, J. Zhu, J. Wang, X. H. Chen, and Y. Zhang, Nature **563**, 94 (2018).

[6] S. Jiang, J. Shan, and K. F. Mak, Nat. Mater. **17**, 406 (2018).

[7] B. Huang, G. Clark, D. R. Klein, D. MacNeill, E. Navarro-Moratalla, K. L. Seyler, N. Wilson, M. A. McGuire, D. H. Cobden, D. Xiao, W. Yao, P. Jarillo-Herrero, and X. Xu, Nat. Nanotech. **13**, 544 (2018).

[8] X. Li, X. Wu, and J. Yang, J. Am. Chem. Soc. **136**, 11065 (2014).

[9] Z. Wang, T. Zhang, M. Ding, B. Dong, Y. Li, M. Chen, X. Li, J. Huang, H. Wang, X. Zhao, Y. Li, D. Li, C. Jia, L. Sun, H. Guo, Y. Ye, D. Sun, Y. Chen, T. Yang, J. Zhang, S. Ono, Z. Han, and Z. Zhang, Nat. Nanotech. **13**, 554 (2018).

[10] D. Zhong, K. L. Seyler, X. Linpeng, R. Cheng, N. Sivadas, B. Huang, E. Schmidgall, T. Taniguchi, K. Watanabe, M. A. McGuire, W. Yao, D. Xiao, K. C. Fu, and X. Xu, Sci. Adv. **3**, e1603113 (2017).

[11] K. L. Seyler, D. Zhong, B. Huang, X. Linpeng, N. P. Wilson, T. Taniguchi, K. Watanabe, W. Yao, D. Xiao, M. A. McGuire, K. C. Fu, and X. Xu, Nano Lett. **18**, 3823–3828 (2018).

[12] L. D. Alegria, H. Ji, N. Yao, J. J. Clarke, R. J. Cava, and J. R. Petta, Appl. Phys. Lett. **105**, 053512 (2014).

[13] M. Mogi, A. Tsukazaki, Y. Kaneko, R. Yoshimi, K. S. Takahashi, M. Kawasaki, and Y. Tokura, APL Mater. **6**, 091104 (2018).

[14] L. Balents, Nature **464**, 199 (2010).

[15] A. Banerjee, J. Yan, J. Knolle, C. A. Bridges, M. B. Stone, M. D. Lumsden, D. G. Mandrus, D. A. Tennant, R. Moessner, and S. E. Nagler, Science **356**, 1055 (2017).

[16] J. M. Kosterlitz and D. J. Thouless, J. Phys. C: Solid State Phys. **6**, 1181 (1973).

[17] W. Zhang, M. B. Jungfleisch, W. Jiang, J. E. Pearson, A. Hoffmann, F. Freimuth, and Y. Mokrousov, Phys. Rev. Lett. **113**, 196602 (2014).

[18] A. K. Nayak, J. E. Fischer, Y. Sun, B. Yan, J. Karel, A. C. Komarek, C. Shekhar, N. Kumar, W. Schnelle, J. Kübler, C. Felser, and S. S. P. Parkin, Sci. Adv. **2**, e1501870 (2016).

[19] S. Nakatsuji, N. Kiyohara, and T. Higo, Nature **527**, 212 (2015).

[20] A. V. Kimel, A. Kirilyuk, A. Tsvetkov, R. V. Pisarev, and T. Rasing, Nature **429**, 850 (2004).

[21] P. Wadley, B. Howells, J. Železný, C. Andrews, V. Hills, R. P. Campion, V. Novák, K. Olejník, F. Maccherozzi, S. S. Dhesi, S. Y. Martin, T. Wagner, J. Wunderlich, F. Freimuth, Y. Mokrousov, J. Kuneš, J. S. Chauhan, M. J. Grzybowski, A. W. Rushforth, K. W. Edmonds, B. L. Gallagher, and T. Jungwirth, Science **351**, 587 (2016).

[22] M. D. Johannes and I. I. Mazin, Phys. Rev. B **77**, 165135 (2008).

[23] V. Brouet, W. L. Yang, X. J. Zhou, Z. Hussain, N. Ru, K. Y. Shin, I. R. Fisher, and Z. X. Shen, Phys. Rev. Lett. **93**, 126405 (2004).

[24] A. Sacchetti, E. Arcangeletti, A. Perucchi, L. Baldassarre, P. Postorino, S. Lupi, N. Ru, I. R. Fisher, and L. Degiorgi, Phys. Rev. Lett. **98**, 026401 (2007).

[25] C. D. Malliakas and M. G. Kanatzidis, J. Am. Chem. Soc. **128**, 12612 (2006).

[26] S. Lei, J. Lin, Y. Jia, M. Gray, A. Topp, G. Farahi, S. Klemenz, T. Gao, F. Rodolakis, J. L. McChesney, C. R. Ast, A. Yazdani, K. S. Burch, S. Wu, N. P. Ong, and L. M. Schoop, Sci. Adv. **6**, eaay6407 (2020).

[27] D. A. Zocco, J. J. Hamlin, T. A. Sayles, M. B. Maple, J.-H. Chu, and I. R. Fisher, Phys. Rev. B **79**, 134428 (2019).

[28] R. Okuma, D. Ueta, S. Kuniyoshi, Y. Fujisawa, B. Smith, C. H. Hsu, Y. Inagaki, W. Si, T. Kawae, H. Lin, F. C. Chuang, T. Masuda, R. Kobayashi, and Y. Okada, Sci. Rep. **10**, 15311 (2020).

[29] M. Watanabe, S.-H. Lee, T. Asano, T. Ibe, M. Tokuda, H. Taniguchi, D. Ueta, Y. Okada, K. Kobayashi, and Y. Niimi, Appl. Phys. Lett. **117**, 072403 (2020).

[30] N. Ru, R. A. Borzi, A. Rost, A. P. Mackenzie, J. Laverock, S. B. Dugdale, and I. R. Fisher, Phys. Rev. B **78**, 045123 (2008).

[31] S. Kim and M. Jung, Appl. Phys. Lett. **112**, 202401 (2018).

[32] Y. Iyeiri, T. Okumura, C. Michioka, and K. Suzuki, Phys. Rev. B **67**, 144417 (2003).

[33] K. Momma and F. Izumi, J. Appl. Cryst. **44**, 1272 (2011).